Calcium Currents in the A7r5 Smooth Muscle–derived Cell Line

An Allosteric Model for Calcium Channel Activation and Dihydropyridine Agonist Action

THEODORE N. MARKS and STEPHEN W. JONES

From the Department of Physiology and Biophysics, Case Western Reserve University, Cleveland, Ohio 44106

ABSTRACT We have investigated the gating kinetics of calcium channels in the A7r5 cell line at the level of single channels and whole cell currents, in the absence and presence of dihydropyridine (DHP) calcium channel agonists. Although latencies to first opening and macroscopic currents are strongly voltage dependent, analysis of amplitude histograms indicates that the primary open–closed transition is voltage independent. This suggests that the molecular mechanisms for voltage sensing and channel opening are distinct, but coupled. We propose a modified Monod-Wyman-Changeux (MWC) model for channel activation, where movement of a voltage sensor is analogous to ligand binding, and the closed and open channels correspond to inactive (T) and active (R) states. This model can account for the activation kinetics of the calcium channel, and is consistent with the existence of four homologous domains in the main subunit of the calcium channel protein. DHP agonists slow deactivation kinetics, shift the activation curve to more negative potentials with an increase in slope, induce intermingled fast and slow channel openings, and reduce the latency to first opening. These effects are predicted by the MWC model if we make the simple assumption that DHP agonists act as allosteric effectors to stabilize the open states of the channel.

INTRODUCTION

Calcium channel gating has generally been described with models containing a series of closed states and an open state. Multiple closed states are required to explain delays in activation kinetics and multi-exponential distributions of channel closed times (Fenwick, Marty, and Neher, 1982). Technical difficulties, particularly the rapid gating kinetics and poor signal to noise ratio at the single channel level, have limited the amount of kinetic information available about calcium channels. Dihydropyridine (DHP) agonists, which improve resolution of channel activity by greatly prolonging

Address reprint requests to Dr. Stephen W. Jones, Department of Physiology and Biophysics, Case Western Reserve University, Cleveland, OH 44106.

J. GEN. PHYSIOL. © The Rockefeller University Press · 0022-1295/92/03/0367/24 $2.00
Volume 99 March 1992 367–390

channel open times (Hess, Lansman, and Tsien, 1984), may provide insights into the normal gating kinetics of calcium channels. However, qualitatively different models of DHP agonist action have been proposed (Hess et al., 1984; Sanguinetti, Krafte, and Kass, 1986; Hering, Kleppisch, Timin, and Bodewei, 1989; Lacerda and Brown, 1989).

Molecular cloning has revealed a large family of proteins that can form sodium, calcium, or potassium channels (Catterall, 1986). Sodium and calcium channel proteins include four repeated homologous domains, each including several putative transmembrane regions. The S4 region, present in each of the four domains, may be the voltage sensor (Noda, Ikeda, Kayano, Suzuki, Takeshima, Kurasaki, Takahashi, and Numa, 1986; Stühmer, Conti, Suzuki, Wang, Noda, Yahagi, Kubo, and Numa, 1989). Homologous potassium channel proteins contain only one such domain, and are thus thought to function as oligomers with four subunits (MacKinnon, 1991).

Recently, Zagotta and Aldrich (1990), Chen and Hess (1990), and Koren, Liman, Logothetis, Nadal-Ginard, and Hess (1990) proposed models for channel gating that involve independent movement of four voltage sensors, as in the original Hodgkin and Huxley (1952) model for potassium channels. However, there was evidence for an additional voltage-independent transition subsequent to movement of the voltage sensors, before channel opening. This is illustrated in Scheme 1 (Fig. 1 *A*). The postulation of four distinct voltage sensors fits well with the structural information, but the nature of the voltage-independent step remained unclear.

We report here data on calcium channel kinetics in the A7r5 smooth muscle–derived cell line. Both single channel and whole cell kinetics have been studied, in the absence and presence of DHP agonists. Under control conditions, the data are well described by Scheme 1. The majority of the data with DHP agonists is consistent with an effect on the closed–open transition in Scheme 1, and no effect on the voltage-dependent steps. However, we find that DHP agonists greatly reduce the latency to first opening of calcium channels (see also Hess et al., 1984; Lacerda and Brown, 1989), which cannot be reproduced by Scheme 1 since most of the latency results from the closed–closed transitions. We also observe both fast and slow components to the open time distribution with DHP agonists, suggestive of multiple open states.

These results can be explained by Scheme 2 (Fig. 1 *B*), based on the Monod-Wyman-Changeux (MWC) model for cooperativity in allosteric proteins such as hemoglobin. Here, movement of a voltage sensor corresponds to binding of a ligand, and the closed and open states correspond to the inactive (T) and active (R) states of the protein. We speculate that depolarization induces small, local conformational changes in the channel protein, presumably movement of the S4 helices. The local changes then facilitate channel opening, which might be a global conformational change involving all domains of the protein. Hille (1984) has also suggested a possible analogy between allosteric enzymes and ion channel gating.

The MWC model may seem complex, with 10 states and 26 rate constants (Fig. 1 *B*). However, the rate constants are determined by relatively few free parameters, given the cyclic nature of the model and our assumptions of symmetry. The kinetics are fully defined at a particular voltage by five parameters (k_C, k_C, k_L, k_{-L}, and f), and one additional parameter defines the voltage dependence. This is only one more

parameter (f) than Scheme 1. More significantly, a state diagram such as Fig. 1 *B* does not do justice to the simplicity of the underlying physical picture, which involves only two states for each voltage sensor (+ and −) and two global conformations of the channel protein (O and C).

The MWC model can reproduce calcium channel activation kinetics both in control and with DHP agonists. Under control conditions, our data are best fit with strong

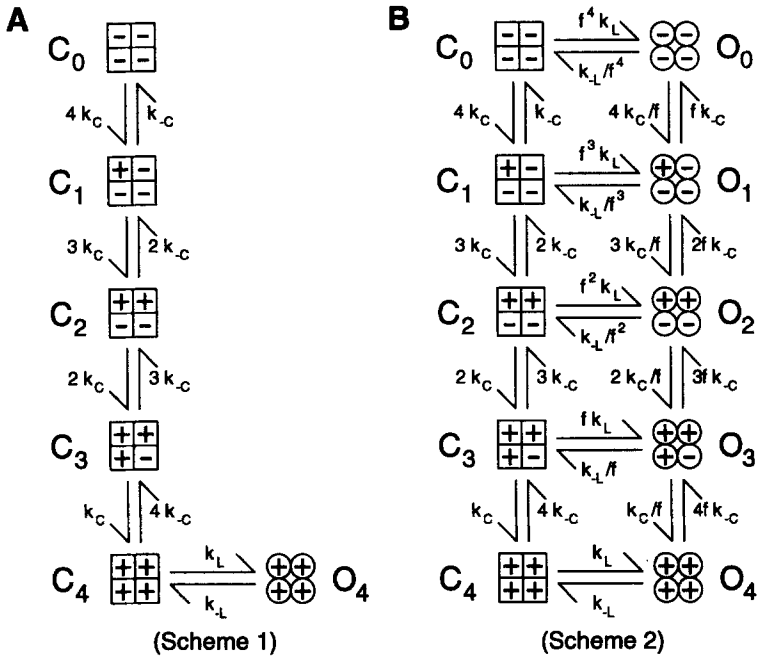

FIGURE 1. Two schemes for calcium channel gating. (*A*) Scheme 1, a linear, six-state model. Vertical transitions reflect movement of a voltage sensor. Horizontal transitions reflect channel opening, which is assumed to be a voltage-independent change in the conformation of the protein. Since the voltage sensors are assumed to be identical, the rate constants within each vertical column are identical except for statistical factors. (*B*) Scheme 2, an adaptation of the MWC model for allosteric proteins to calcium channels. Voltage-independent transitions between closed and open states are theoretically possible with any number of voltage sensors moved, but are much more likely with an increasing number of sensors in the + position. The factor f relates rate constants for the movement of a voltage sensor in the closed conformation to those in the open state, as well as the voltage-independent rate constants with different numbers of voltage sensors moved. The voltage sensors move from the − to the + position more readily when the channel is in the open state.

cooperativity, where the MWC model reduces to Scheme 1. We propose that DHP agonists act as allosteric effectors to stabilize the open state, much as 2,3-diphosphoglycerate acts to stabilize the T state of hemoglobin. With DHP agonists, the shift in the closed–open equilibria weakens the cooperativity sufficiently to allow openings to the O_3 state.

METHODS

Cells

A7r5 cells were acquired from American Type Culture Collection (Rockville, MD) and grown in Dulbecco's modified Eagle's medium with 10% calf serum (CS) added. After cells reached confluence, serum was reduced to 0.5%. Cells were maintained on 0.5% CS for 1–3 wk. Quiescent cells were trypsinized and replated with cytochalasin (1 μg/ml) to prevent the normal flattening and spreading on the dish. The cytochalasin-treated cells maintained an obviously round morphology with few processes for up to 2 d after replating.

Single Channel Recording

Currents were recorded using an EPC-7 patch clamp amplifier (List Electronic, Darmstadt, Germany). Voltage commands were given and data were collected using an AT-type computer, pCLAMP software (v. 5.5), and a Labmaster A-D converter. Electrodes of ~5 MΩ were drawn from borosilicate glass (World Precision Instruments, Sarasota, FL) and coated with silicone rubber. The pipette solution contained (mM): 90 $BaCl_2$ and 10 K-HEPES, pH 7.4. After seals were formed in a physiological salt solution, the cell membrane potential was zeroed with a bath solution containing (mM): 120 KCl, 10 K-EGTA, and 10 K-HEPES, pH 7.4. The bath solution was superfused by gravity feed. BAY K 8644 and (+) 202-791 were introduced into either the bath or the pipette solution.

The incoming analog signal was filtered at 1 or 3 kHz and digitized at 2 or 10 kHz, respectively. Sweeps with no openings were subtracted from those with openings in order to cancel capacitative transients and leak currents. During analysis the data were filtered with a digital Gaussian filter (0.3–2.5 kHz). 50% threshold-crossing routines included in Fetchan were used for event detection.

Most patches analyzed in detail (Figs. 2–5, 7, 11, 12) contained only one channel, based on the lack of overlapping openings (Horn, 1991), even in the presence of DHP agonists, where the probability of being open (p(open)) is high and most sweeps show channel activity.

Amplitude Histograms

Under control conditions, gating kinetics within a burst were too rapid to be resolved directly (see Results). A modification of the method of Yellen (1984) and FitzHugh (1983) was used to estimate rate constants for channel opening and closing from point-by-point amplitude histograms. Ideally, the amplitude histogram for a channel showing simple two-state (closed–open) kinetics, when filtered heavily, is described by a beta distribution:

$$f(x) = x^{(a-1)}(1 - x)^{(b-1)} \quad (1)$$

where $a = k_L\tau$, $b = k_{-L}\tau$, x is the current amplitude (on the scale 0 = closed, 1 = open), k_L and k_{-L} are the opening and closing rates, and τ is the cutoff frequency of the filter. The effect of recording noise can be incorporated by convolving the beta distribution with a Gaussian, fit to the baseline noise (0.07–0.1 pA after 300-Hz Gaussian filtering in our experiments). Amplitude histograms included only points within bursts, defined as times when the current was >25% of the full open channel amplitude (measured after addition of a DHP agonist) for ≥2 ms. Since the rising and falling edges of each burst are distorted by filtering, the first and last 1 ms of each burst were not used (the 10–90% rise time of a 300-Hz Gaussian filter is ~1.2 ms). This analysis was done with programs written by the authors in QuickBASIC.

Whole Cell Currents

The signal was analog filtered at 25 kHz before digitization at either 20 or 100 kHz. Cell capacitance (15–35 pF) and series resistance (2.5–5.0 MΩ) were determined by optimal transient cancellation. Series resistance was compensated 60–70%. This results in a theoretical time constant for voltage clamp <0.1 ms, and a steady-state voltage error of ~ 2 mV with 1 nA of current. Often an additional transient component which was difficult to cancel was observed, possibly representing capacitance of membrane infoldings (e.g., T tubules). Otherwise, space clamp presents little problem in these cells as they are spherical with diameters <40 μm. Leak current was corrected for by averaging, scaling, and adding four steps of amplitude -0.25 of the test step. The pipette solution contained (mM): 120 CsCl, 4 $MgCl_2$, 5 $Tris_2$-ATP, 1 Cs_2-EGTA, and 2.5 Cs-HEPES, pH 7.2. To maintain consistency with single channel experiments, the bath solution contained (mM): 90 $BaCl_2$ and 10 NMG-HEPES, pH 7.4.

Strategy for Modeling

Two models will be considered in detail: a linear six-state scheme (Scheme 1) and the MWC model (Scheme 2) (Fig. 1). We will argue below that simpler models (such as C-C-O or Hodgkin-Huxley-type models) cannot fit important features of our data. Data in control conditions and with DHP agonists will be discussed in parallel, since we conclude that the effects of DHP agonists can be explained by a relatively simple modification of normal gating kinetics. Inactivation (Giannattasio, Jones, and Scarpa, 1991) will not be considered here.

Both models assume that the channel contains four identical voltage sensors, which move independently (except for the cooperativity introduced by closed–open transitions). Scheme 1 thus is determined by four parameters (k_C, k_C, k_L, and k_{-L}) at a given voltage. We will assume that the rate constants for movement of each voltage sensor depend exponentially on voltage (Stevens, 1978), with equal voltage dependence for movement of the sensor in each direction:

$$k_C = Ae^{(V/V_S)}, k_{-C} = Be^{(-V/V_S)} \tag{2}$$

where A and B are the rate constants at 0 mV, and V_S is inversely proportional to the equivalent charge moved across the membrane field between a state and a transition state. These assumptions mean that the microscopic voltage dependence of the model is determined by a single parameter, the amount of charge moved by one voltage sensor.

To reduce the number of free parameters on the MWC model, we assume symmetrical changes in the voltage-dependent transitions both between closed and open states, and between the closed–open rate constants for transitions with different numbers of voltage sensors moved. Those assumptions mean that the MWC model is determined by one free parameter, f, in addition to those in Scheme 1. The parameter c in the original Monod, Wyman, and Changeux (1965) model is equal to f^2. We also assume that the action of DHP agonists can be explained by symmetrically increasing k_L and decreasing k_{-L} by the same factor, Δ_{DHP}.

The order in which the data are presented below corresponds roughly to the sequence used for determination of the model parameters. The rate constants for channel opening and closing in control conditions (k_L, k_{-L}) are determined primarily by channel gating during bursts. Information about closed–closed transitions (k_C, k_{-C}) depends in part on the steady-state activation curve (which determines the ratio, k_C/k_{-C}, and the voltage dependence). The shift in the activation curve with DHP agonists sets the factor by which k_L and k_{-L} are changed. The kinetics of whole cell currents determine the absolute magnitudes of k_C and k_{-C}. The parameter f, which strongly influences the cooperativity, is not directly determined by the data, but constraints on f are discussed below.

One difficulty that we encountered was the lack of a general method for fitting a model to

data when qualitatively different sorts of data are involved (e.g., single channel and whole cell experiments). We resorted to an iterative process based heavily on simulations, where we guessed a set of rate constants, simulated whole cell currents with realistic series resistance, and simulated single channels with realistic noise. We used modified versions of AXOVACS programs for whole cell currents, and CSIM (Axon Instruments, Inc., Foster City, CA) for single channels. We then analyzed the simulated data as we would real data, including filtering. Next, the rate constants were changed based on any discrepancies between model and experimental data, and the entire cycle was repeated.

RESULTS

Single Channel Currents

Activation of calcium channels is clearly voltage dependent (Fig. 2 *A*). Under control conditions, openings are rare and brief at negative voltages. At positive voltages, openings occur mostly in bursts. Channel opening events with DHP agonists are more frequent and longer, with "tail" events indicating a slow channel closing rate even at −80 mV. Bursts are longer and more frequent at more positive potentials.

To determine whether the open channel conductance was the same for control and DHP-stimulated channels, we examined the relationship between event duration and amplitude at 0 mV, where the signal to noise ratio is most favorable. It is clear from Fig. 2 *A* that the open channel current is easily measurable with DHP agonists, but most openings in control are attenuated. Fig. 2 *B* shows that the longest events in control have amplitudes comparable to those with DHP agonists, suggesting that the true open channel current is the same under both conditions.

With DHP agonists, the conductance is nearly linear with voltage in the measurable region (Fig. 2 *C*). In this patch, the conductance was 20 pS with an extrapolated reversal potential of +54 mV.

Amplitude Histograms

Direct measurements of channel open and closed times using threshold-crossing analysis yielded a single mean open time of ~0.3 ms and multiple closed times, with most closed times falling in the most rapid distribution of $\tau \approx 0.2$ ms. We consider those values to be completely unreliable, as the heavy filtering needed for a favorable signal to noise level (~1 kHz, dead time = 0.18 ms) distorts the signal to the extent that too many events would be missed.

We attempted to study channel gating with noise analysis (data not shown). There was a clear difference between power spectra of active and null sweeps, but difference spectra were fit poorly by a single Lorentzian. A component with τ = 1–4 ms could be detected at some voltages (generally −10 to +10 mV), probably corresponding to the duration of a burst of openings. There was excess noise at higher frequency, but it could not be uniquely fit to a second Lorentzian, as the difference between spectra of active and null sweeps became undetectable above 1 kHz even when many sweeps (~50) were averaged. At more positive voltages, or with DHP agonists, power spectra could be approximated as $1/f$ noise, probably due to the superimposition of several Lorentzians resulting from gating and bursting over a wide range of time scales.

We next considered point-by-point amplitude histograms (Fig. 3), which contain

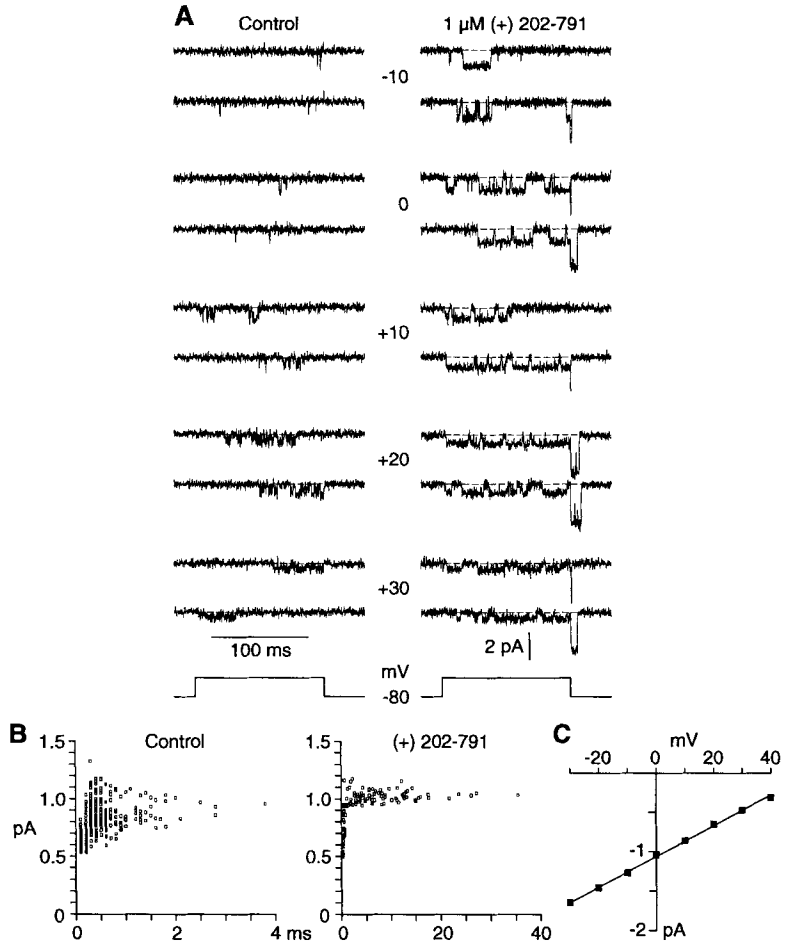

FIGURE 2. (*A*) Gating of single calcium channels in A7r5 cells. Depolarizing steps (135 ms) were given at 2-s intervals. (+) 202-791 was added to the bath. These traces were digitally filtered at 1,500 Hz on final analysis. (*B*) Measured single channel current amplitudes as a function of event duration. Traces at 0 mV were filtered at 1,000 Hz and events were detected using a threshold-crossing routine. (*C*) Single channel currents between −30 and +40 mV in the presence of (+) 202-791. Peaks of the point-by-point amplitude histograms were fit by eye to determine the open channel current. Data in this figure are from patch b9d20.

information on rapid kinetic processes (Yellen, 1984). Within bursts of channel activity, most points were considerably below the full open channel amplitude. This confirms the visual impression (Fig. 2 *A*) that channel gating within a burst is extremely fast, so that the recorded channel amplitude is usually a weighted average of the true closed and open channel amplitudes. Although there is noticeable variation from channel to channel (Fig. 3), in all three patches the peak of the distribution is at 0.5–0.7 of the open channel current. Furthermore, the peak did not shift with voltage over a 20–30-mV range. This indicates that gating within a burst is

not detectably voltage dependent (see Fig. 2 *A*). In terms of Schemes 1 and 2, the voltage independence of gating within a burst suggests that the microscopic channel opening step does not involve movement of a significant amount of charge.

To explore this further, we compared amplitude distributions from experimental data, simulated data, and beta distributions (Fig. 4). The position of the experimental peak along the amplitude axis, and the shape of the curve, are well fit by a beta distribution with $k_L = 12\ ms^{-1}$ and $k_{-L} = 6\ ms^{-1}$. Changes in the equilibrium constant shift the position of the peak (Fig. 4 *A*). The simulated data, using the rate constants

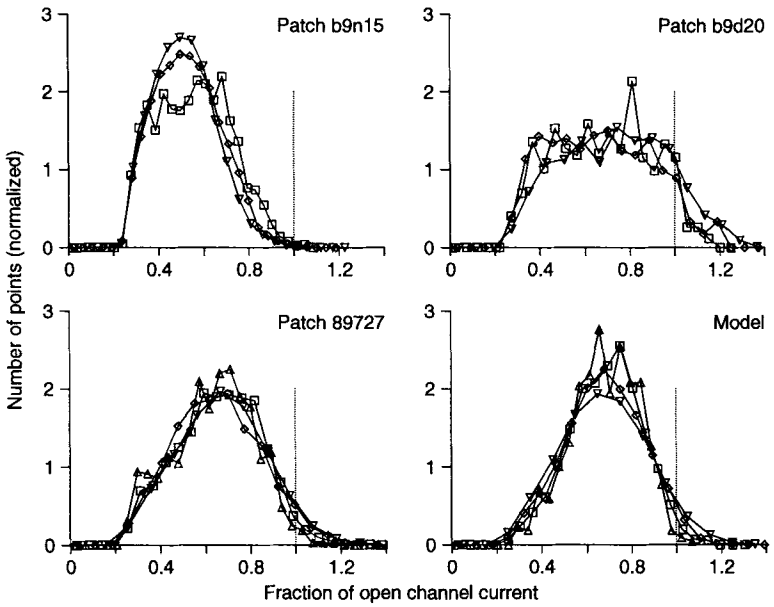

FIGURE 3. Analysis of point-by-point amplitude histograms during bursts. Histograms were binned in 0.05-pA intervals, and are shown with currents normalized to the open channel current measured with 1 μM (+) 202-791 or BAY K 8644 at each voltage in each patch. The histograms were also normalized to give an integral of 1. Currents were recorded at −10 mV (△), 0 mV (□), +10 mV (◇), and +20 mV (▽). The vertical dotted lines emphasize the observation that the recorded current was almost always less than the true open channel current. Bursts were defined as described in Methods. At the lower right are histograms generated from simulation of Scheme 2 using the parameters given in Table III.

described below for closed–closed transitions to produce realistic bursting, are also well fit by beta distributions (Fig. 4, *A–C*), and the simulated amplitude distributions are not voltage dependent (Fig. 3, lower right). This suggests that our assumptions about closed–closed kinetics and our criteria for identifying bursts are not critical here. The distributions depend strongly on the equilibrium constant (Fig. 4, *A* and *B*), and are reasonably sensitive to the absolute rate constants (Fig. 4 *C*). A threefold slowing of kinetics is clearly distinguishable, but threefold faster gating produces a distribution that is only slightly narrower. In theory, the width of the distribution

should change with voltage due to changes in the signal to noise ratio, but that was not consistently observed (Fig. 4 *D*; see also Fig. 3).

Gating with DHP Agonists

In the presence of DHP agonists, most openings appear long enough to be well resolved at a 1-kHz bandwidth. However, very fast events, both openings and closings, were also observed. Good fits to open time distributions in the presence of 1

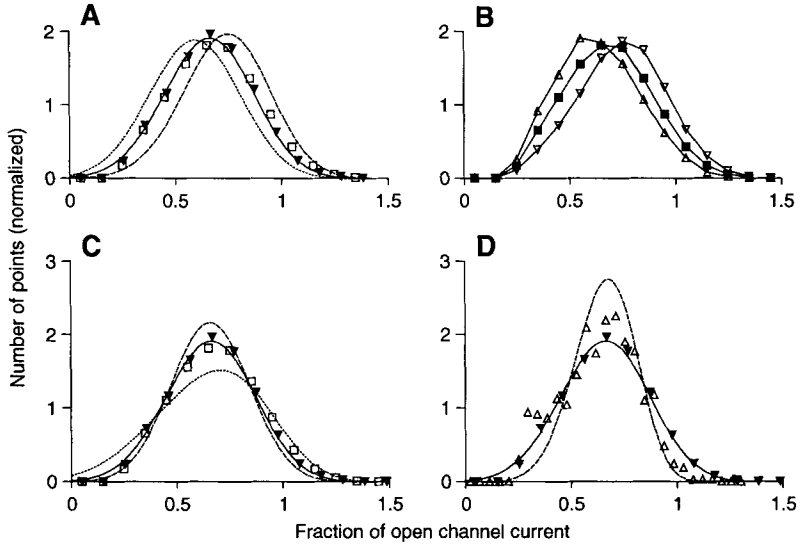

FIGURE 4. Comparison of amplitude histograms to beta distributions. (*A*) The effect of changes in the closed–open equilibrium. The smooth curves are beta distributions calculated for k_L = 10.8 and k_{-L} = 7.2 (dotted lines), k_L = 12 and k_{-L} = 6 (solid lines), and k_L = 13.5 and k_{-L} = 4.5 (dashed lines) for equilibrium constants (k_L/k_{-L}) of 1.5, 2, and 3, respectively. Solid triangles are experimental data within bursts (cell 727, +20 mV); open squares are simulated from Scheme 2 (Table III). (*B*) Data simulated from Scheme 2 at +20 mV for k_L and k_{-L} values as in *A*. (*C*) The effect of changes in absolute rate constants, with k_L/k_{-L} = 2. The dashed line is k_L = 36 and k_{-L} = 18, the solid line is k_L = 12 and k_{-L} = 6, and the dotted line is k_L = 4 and k_{-L} = 2. Experimental data (solid triangles) and simulations (open squares) as in *A*. (*D*) Comparison of experimental data (symbols) to beta distributions calculated from Scheme 2 (Table III) (lines) for −10 mV (open triangles and dashed line) and +20 mV (solid triangles and solid line).

μM (+) 202-791 require at least two exponentials. Although the fast component (τ ~0.3 ms) is poorly quantified given the limited bandwidth, its presence is clear. The time constants for both the fast and slow open events appear to be voltage independent between −10 and +10 mV (Fig. 5 *A*). Qualitatively, this is as expected from Scheme 2. Although Scheme 2 does predict some voltage dependence for open durations due to the voltage-dependent transition between O_3 and O_4, simulations show this to be negligible between −20 and +20 mV.

The distribution of closed times was complex, but the more rapid closing events were not obviously voltage dependent (Fig. 5 *A*). The occasional observation of very rapid closings in single channel currents after repolarization to negative potentials (Fig. 5 *B*) also suggests that the primary closed–open reaction is voltage independent, as a voltage-dependent opening would almost never occur at −80 mV. For one channel at 3-kHz bandwidth, a single exponential fit to closed times at −80 mV gave τ = 64 μs, which must be inaccurate as it is barely longer than the 60 μs dead time of

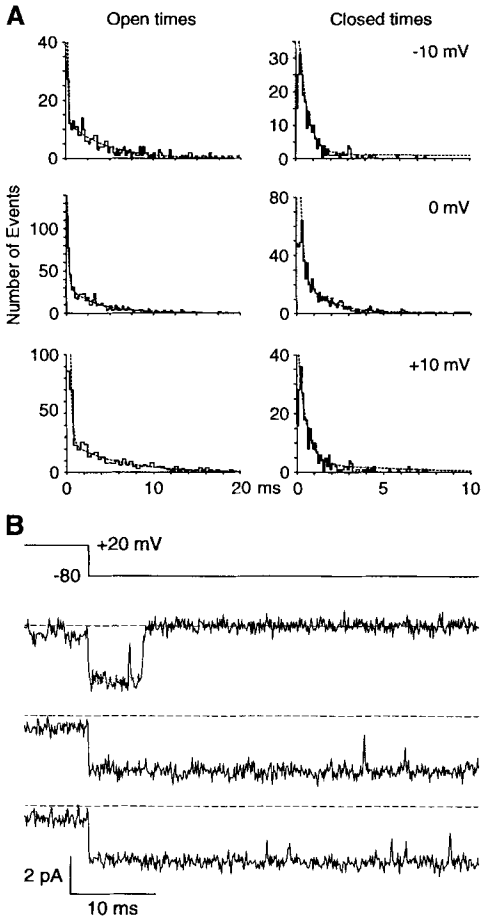

FIGURE 5. Kinetics of DHP-modified calcium channel gating. (*A*) Distributions of dwell times in the presence of 1 μM (+) 202-791. Dashed lines are fits to the sum of two exponential distributions. The slower open time constants were 9.2 ms (−10 mV), 8.6 ms (0 mV), and 6.0 ms (+10 mV). (*B*) Single channel tail currents on repolarization to −80 mV show fast closing events. *A* and *B* are from patch b9d20.

the filter. Similar brief closings were observed in other patches, but there were too few tail events to attempt to measure time constants. Scheme 2 predicts that reversible closings at −80 mV must be brief, as k_L is very fast in the presence of DHP agonists. At −80 mV most detectable closings will be followed by "irreversible," voltage-dependent closed–closed transitions rather than by reopenings. The long open times during single channel tail currents (Fig. 5 *B*) resemble those observed at more depolarized potentials, but the problems with missed closing events preclude a quantitative analysis.

A bi-exponential distribution of open times is not consistent with the linear six-state model (Scheme 1), and simulations using such a scheme yield only a single open time distribution, regardless of missed closing events. Thus, there must be at least two open states in the presence of DHP agonists. The MWC model can explain a population of short openings as transitions from C_3 to O_3. As the channel is very likely to be in state C_3 immediately before and after a burst, the MWC model predicts that the shorter openings should occur preferentially, although not exclusively, in close temporal relation to bursts.

An alternate interpretation is that the short openings are to the normal open state, and the long openings are of the DHP-modified channel. We examined the concentration dependence of DHP action to test that possibility. If binding and unbinding of DHP agonists is rapid, short and long openings will be intermingled, but the channel open time(s) might be concentration dependent (Lacerda and Brown, 1989). If DHP binding is slow, concentration dependence would be reflected in sweep-by-sweep changes in channel activity rather than in gating kinetics on the millisecond time scale (Hess et al., 1984).

Concentration Dependence of DHP Agonist Action

As the concentration of DHP agonist was increased from 10 nM to 100 nM to 1 μM, an increasing number of sweeps with long openings was observed (Fig. 6 *A*). No long openings were observed in the absence of drug in this patch. A complex distribution of open times is evident from Fig. 6 *A*. Bi-exponential fits to open time histograms for this patch and two others reveal that the time constants are not detectably concentration dependent, but the relative number of short and long openings changes in a concentration-dependent manner (Table I).

We examined p(open) in each sweep that had at least one long (>3 ms) opening, as a function of DHP agonist concentration. If binding and unbinding are rapid with respect to the test pulse length (135 ms), then increasing the concentration should increase p(open) within a sweep, as DHP rebinding is more likely to occur at high concentrations. Conversely, if binding and unbinding are slow with respect to the sweep length, sweeps showing long openings should have the same p(open) regardless of concentration, as it is unlikely that association or dissociation will occur over the time of the test pulse. There was a wide range of p(open) among sweeps with long openings at all concentrations (Fig. 6 *B*). Only a few sweeps contained openings longer than 3 ms in control, and their mean p(open) was relatively low. The mean p(open) for sweeps with long openings was virtually the same at all DHP agonist concentrations (Fig. 6 *B*), despite a fivefold increase in the number of sweeps with long openings (Fig. 6 *C*).

If binding and unbinding were very slow (τ on the order of seconds), then we expect sweeps with long openings to be consecutive at low DHP agonist concentration. We do not observe this consistently (Fig. 6 *A*), which argues against very slow kinetics. Clearly, most if not all of the concentration dependence of the effect of DHP agonists appears as changes in gating from sweep to sweep, consistent with relatively slow binding and unbinding, on the order of hundreds of milliseconds.

Sweeps selected to have long openings also contain an excess of short openings (Fig. 7 *A*). Qualitatively, inspection of records in the presence of DHP agonists at

weak depolarizations reveals that the short openings can appear in close proximity to long openings (Fig. 7 *B*), as expected from Scheme 2 (Fig. 7 *C*). We conclude that DHP-modified channels have access to at least two open states.

Channel gating kinetics with DHP agonists help define the cooperativity factor f. Extremely strong cooperativity ($f \ll 1$) reduces the model to Scheme 1, and weak

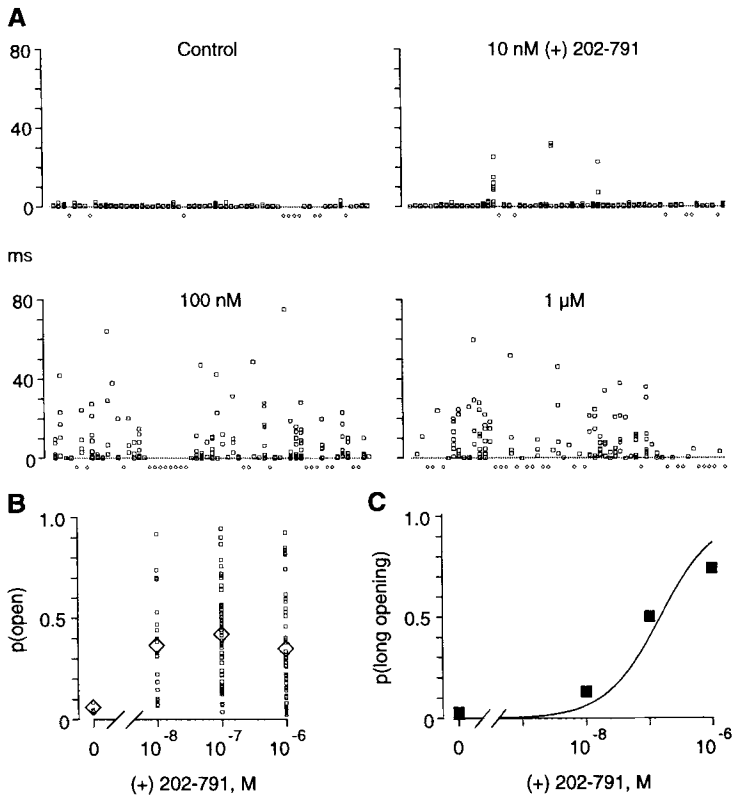

FIGURE 6. Concentration dependence of DHP-modified gating. (*A*) All measured open times are plotted on a sweep-by-sweep basis in control and in different (+) 202-791 concentrations. Patch a9815. (*B*) The probability of being open was measured during each sweep that produced at least one opening longer than 3 ms. Squares represent the p(open) in individual sweeps and diamonds represent the mean p(open). (*C*) The proportion of active sweeps with at least one long (>3 ms) opening at different (+) 202-791 concentrations. The solid line is drawn according to the law of mass action for a single DHP binding site with K_d = 150 nM. *B* and *C* are from patch a9907.

cooperativity ($f \approx 1$) produces a voltage-independent channel. With $f = 1/15$, channel gating with DHP agonists was well reproduced. A twofold increase in f produces too many fast openings, and a twofold decrease in f practically eliminates openings to the O_3 state.

Whole Cell Currents

Properties of whole cell currents in these cells with lower concentrations of Ba^{2+} and Ca^{2+} have been reported (Galizzi, Qar, Fosset, Van Renterghem, and Lazdunski, 1987; Van Renterghem, Romey, and Lazdunski, 1988; Fish, Sperti, Colucci, and Clapham, 1988; McCarthy and Cohen, 1989). In our hands most A7r5 cells express DHP-sensitive calcium current predominantly (Marks, Dubyak, and Jones, 1990), although a significant amount of rapidly inactivating, low threshold T-type current was occasionally present. There was no evidence for T current in the cells analyzed here. High external Ba^{2+} concentrations shifted the current–voltage curves in the positive direction, probably due to a surface charge effect.

Examples of currents evoked by steps to +20 mV in the absence and presence of

TABLE I

Concentration Dependence of (+) 202-791 Effects on Channel Open Times

Cell	[(+)]292-791]	No. of events	τ_1	A_1	τ_2
	nM		*ms*		*ms*
a9810	0	473	0.27	1.00	
	10	356	0.30	0.79	13.3
	100	222	0.28	0.76	10.7
	1,000	551	0.26	0.64	5.7
a9815	0	786	0.26	1.00	
	10	121	0.20	0.92	2.4
	100	88	0.17	0.69	3.8
	1,000	547	0.34	0.50	2.3
a9907	0	650	0.29	1.00	
	10	698	0.27	0.91	6.4
	100	661	0.35	0.71	9.9
	1,000	200	0.20	0.32	17.6

Channel openings were measured at 0 mV and filtered at 1 kHz. Data were fit to a single exponential (0 nM) or the sum of two exponentials (10–1,000 nM). A_1 is the fraction of opening events in the more rapid distribution (τ_1). Data are not corrected for missed events.

(+) 202-791 are shown in Fig. 8 *A*, with current–voltage relationships for the same cell in Fig. 8 *B*. To estimate the steepness of the voltage dependence of opening and the voltage of half-maximal activation, we fitted the currents empirically to a Boltzmann function:

$$I(V) = Ni\{1 + \exp[(V_{0.5} - V)/K]\}^{-1} \quad (3)$$

where N is the number of channels open at extreme positive potentials, i is the single channel current at the test potential V, $V_{0.5}$ is the voltage of half-maximal activation, and K is inversely related to the steepness of the voltage dependence. At potentials greater than +30 mV we noticed variability both among cells and in the same cell over the course of the experiment, possibly due to small errors in leakage subtrac-

tion. We therefore confined the analysis to potentials between −40 and +30 mV, a range where the single channel conductance is linearly dependent on voltage (Fig. 2 *C*). Addition of (+) 202-791 shifted $V_{0.5}$ to more negative voltages, decreased K, and increased N (Table II).

Naively, the increase in N would indicate that DHP agonists increase the number of available calcium channels. Instead, we interpret the effect as primarily an increase in the saturating level of p(open) reached at extreme positive potentials. The MWC model, with our parameters, predicts that p(open) at positive voltages will approach

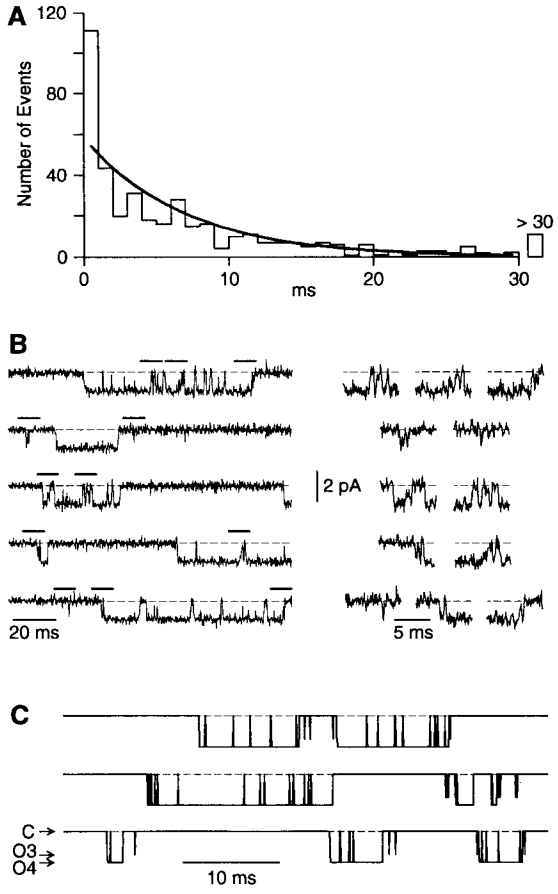

FIGURE 7. Short and long openings are temporally related with DHP agonists. (*A*) A histogram of opening events at 0 mV in sweeps with at least one opening ≥3 ms. The thick line is the distribution expected for a single exponential with time constant equal to the average open time (6.85 ms). (*B*) Five consecutive sweeps with openings at −10 mV. Regions under the solid lines are shown on an expanded time scale (right). *A* and *B* are from patch b9d20, in 1 μM (+) 202-791, filtered at 1 kHz (*A*) or 1.5 kHz (*B*). (*C*) The MWC model predicts that fast openings will be frequently found in association with bursts. Although we assume that the states O_3 and O_4 have the same conductance, they are shown here at different amplitudes to allow for visual discrimination.

the voltage-independent p(open) during a burst, which is ~0.67 in control and ~1 with DHP agonists. It is possible that DHP agonists also affect the amount of inactivation, which would appear as a change in N.

In cases where the voltage clamp was of good enough quality to accurately measure tail currents, the shape of the activation curve determined from tail currents agreed well with the relative conductance measurements described above (Fig. 8 *C*). Relative conductance values for five cells in the absence and presence of (+) 202-791 are plotted in Fig. 9 along with a fit using the MWC model. Since the increase in maximal

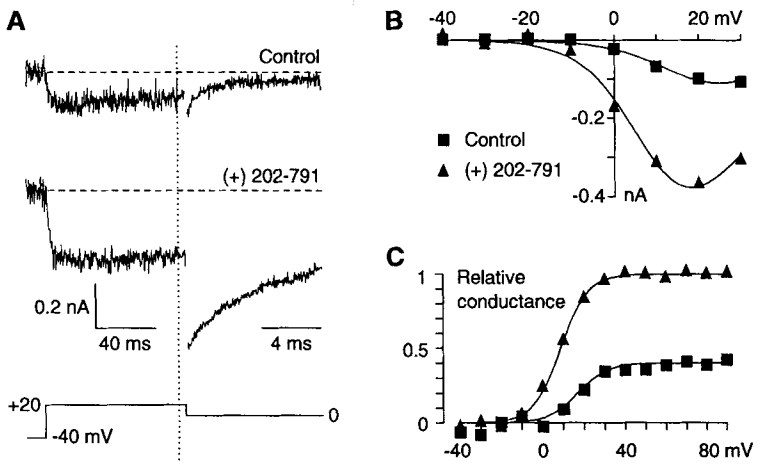

FIGURE 8. Whole cell currents in the absence and presence of (+) 202-791. (*A*) Inward currents before and after addition of 1 μM (+) 202-791 to the bath. Currents to the left of the vertical dotted line were digitized at 10 kHz and filtered at 1 kHz, and those to the right were digitized at 100 kHz and filtered at 5 kHz. (*B*) Current–voltage relationship. Squares are in control conditions and triangles are after addition of 1 μM (+) 202-791 to the bath. Steady-state currents were measured at the end of 50-ms pulses. The solid lines are fits between −40 and +30 mV using a Boltzmann function (Eq. 3) and assuming a linear single channel current–voltage relationship (Fig. 2 *C*). (*C*) Activation curves measured from tail currents. The solid lines are drawn according to the same Boltzmann functions as in *B*. Tail currents were measured 400–550 μs after repolarization to 0 mV. Since tail current measurements in control and (+) 202-791 cannot be directly compared, values were scaled to a maximum of 1 for (+) 202-791 and 0.4 for controls, to correspond to the relative conductances (*N*) of the Boltzmann functions in *B*. Cell a0124.

conductance with DHP agonists was variable, in part due to rundown, conductances were normalized to 1 in the presence of (+) 202-791 and to 0.667 for controls.

The steady-state activation curve provides information on the voltage-dependent steps in the MWC model. $V_{0.5}$ is strongly affected by the ratio of the rate constants describing the movement of a single voltage sensor within a closed channel, and the steepness is a function of the charge moved in association with each voltage sensor (which depend on A/B and V_s, respectively, Eq. 2). The activation curve was well fit with A/B = 0.62 and V_s = 26 mV, or approximately two elementary charges per voltage sensor (Fig. 9). The changes in $V_{0.5}$ and K with (+) 202-791 were modeled as a 12.25-fold change in the equilibrium constant for each of the voltage-independent

TABLE II

Effects of (+) 202-791 on Activation of Whole Cell Calcium Currents

	Change in N	$V_{0.5}$	K
Control	—	17.5 ± 2.2	7.5 ± 0.2
1 μM (+)202-791	2.2 ± 0.2	3.1 ± 2.2	5.7 ± 0.3

N, $V_{0.5}$, and K are defined in Eq. 3; here, N is normalized to the value found without (+) 202-791. Values are means ± SE, n = 5.

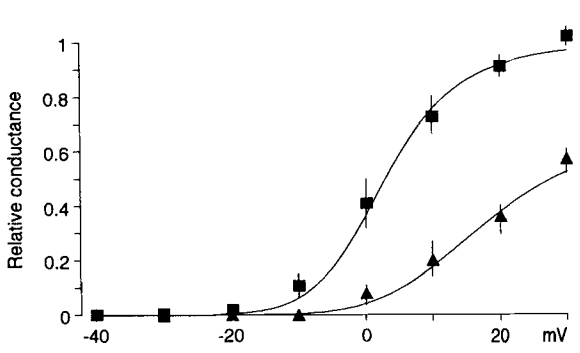

FIGURE 9. Steady-state activation curves fit with the MWC model. Whole cell currents from five cells were fit as in Fig. 8 *B*, for data in the absence (triangles) and presence (squares) of 1 μM (+) 202-791. The relative conductance was normalized to 1 for (+) 202-791 and 0.667 for control data. The solid lines are fits using the MWC model with $A/B = 0.62$ and $V_S = 26$ mV.

C − O steps. Note that the changes in macroscopic voltage dependence with DHP agonists, including a change in the steepness of the activation curve, can be explained fully with no effect of DHP agonists on the voltage sensors themselves.

Absolute values for A and B can be obtained from kinetic data. In control conditions, activation can be well fit using a Hodgkin-Huxley style model with $n = 4$. This is expected from the MWC model as long as most of the openings are to O_4 (i.e., strong cooperativity), and the $C_4 - O_4$ transition rates are much faster than the voltage-dependent transition rates between closed states. We determined the coefficients for closed-channel voltage sensor movement by fitting the model by eye to control whole cell activation kinetics, constraining the ratio A/B to be 0.62: $A = 0.26$ ms^{-1} and $B = 0.38$ ms^{-1} (Fig. 10). The change in the voltage-insensitive equilibrium constants caused by (+) 202-791 was assumed to involve an increase of the opening

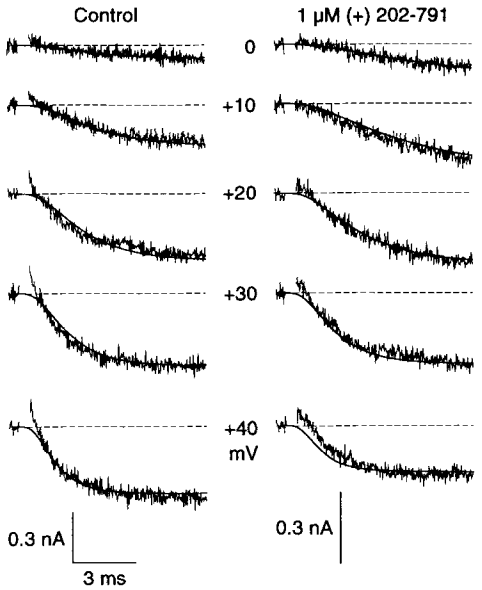

FIGURE 10. The time course of whole cell currents fit with the MWC model. The noisy traces are currents resulting from 10-ms steps from a holding potential of −40 mV to the indicated test potentials in control (left) and with 1 μM (+) 202-791 (right). 500 μs after each voltage step was blanked. Currents calculated from the MWC model ($A = 0.38$, $B = 0.26$) are superimposed.

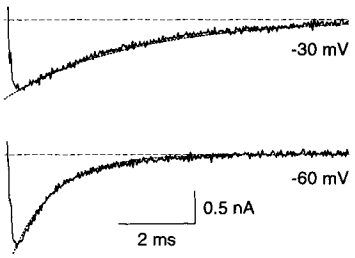

FIGURE 11. Tail currents with 1 μM (+) 202-791. The noisy traces are tail currents on repolarization to indicated potentials after steps to +50 mV, with tail currents simulated using the MWC model superimposed (dashed lines). Filtered at 5 kHz.

rates and a decrease of the closing rates, each by a factor of 3.5 (i.e., $k_L = 42$ and $k_{-L} = 1.71$ ms^{-1}).

At negative voltages, tail currents in control conditions were generally too fast to be accurately clamped. However, DHP-modified tail currents can be measured in well-clamped cells. Tail currents in the presence of 1 μM (+) 202-791 show a clear dependence on voltage, and are usually well fit with a single exponential decay. The MWC model, with parameters described above, accurately simulates tail currents with

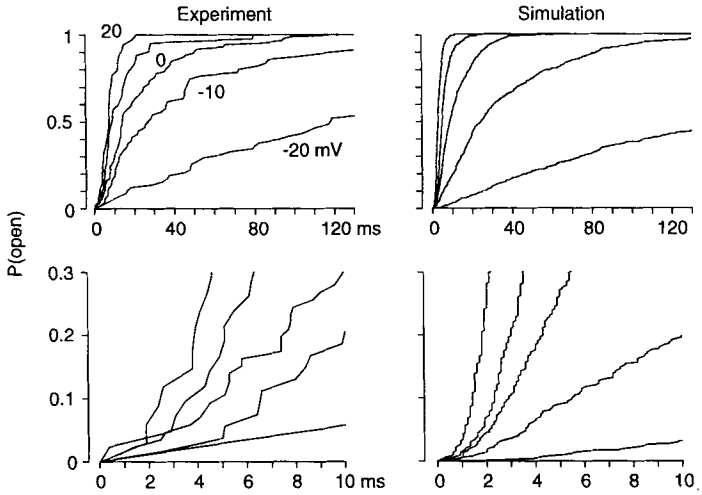

FIGURE 12. Latencies to first opening are strongly voltage dependent. (*Left*) Cumulative plots of first latencies with 1 μM (+) 202-791. The holding potential was −80 mV and test potentials were −20, −10, 0, +10, and +20 mV. Events were detected by threshold crossing, with digital filtering at 1,000 Hz (−20 to 0 mV) and 300 Hz (+10 and +20 mV). The number of events at each voltage were 31 (−20), 49 (−10), 87 (0), 43 (+10), and 34 (+20). At voltages where saturation was apparent (≥0 mV) the data were normalized to a p(open) of 1.0, on the assumption that null sweeps result primarily from sweeps spent in an inactivated state. In this patch (b9d20), measured probabilities at saturation were 0.64 (0 mV), 0.56 (+10 mV), and 0.453 (+20 mV). At potentials where saturation was not evident, the data were normalized to the average p(open) from the more depolarized traces, 0.55. Data at early times are shown on an expanded scale below. (*Right*) Simulated first latency distributions. 500 sweeps were simulated for each potential. The voltages used for the simulations were shifted 5 mV in the depolarized direction to agree better with this patch. Simulated data were analyzed in the same manner as the experimental data, including filtering and addition of simulated noise.

TABLE III

Parameters Used in Simulations of the MWC Model

k_L	k_{-L}	A	B	V_s	f	Δ_{DHP}
ms^{-1}	ms^{-1}	ms^{-1}	ms^{-1}	mV		
12	6	0.26	0.38	26	1/15	3.5

DHP agonists (Fig. 11). Simulations of control conditions produce tail currents with fast time constants (e.g., $\tau \approx 200$ μs at −40 mV).

The data from whole cell experiments define the voltage-dependent rate constants for closed–closed transitions. As the value of f was fixed above, defining the microscopic rate constants for the movement of a voltage sensor in a closed channel also serves to determine the rate constants for the sensor moving in an open channel. Table III summarizes the parameters used for simulations based on the MWC model.

Distribution of Latencies to First Opening

The first latency distribution provides an independent picture of the voltage dependence of channel gating. Since latencies reflect the rate of movement of the channel through closed states, they are expected to be strongly voltage dependent. As event detection is more reliable when the channels are DHP modified, we were able to measure first latencies over a 40-mV range in the presence of (+) 202-791. The cumulative latency plots rise in a voltage-dependent manner after a brief but clear delay (Fig. 12). Simulations with the MWC model using the rate constants derived above show similar kinetics, including the delay (Fig. 12).

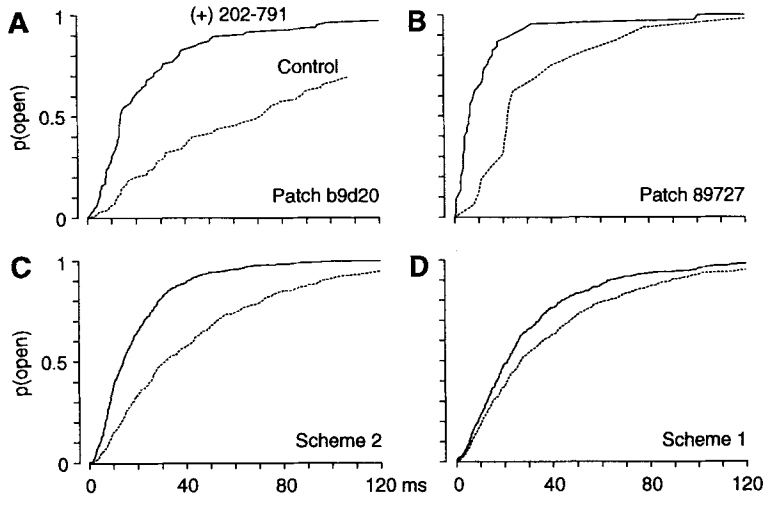

FIGURE 13. DHP agonists shorten latencies to the first opening. (*A*, *B*) Latencies to first opening at 0 mV from two separate experiments before (solid line) and after (dashed line) addition of DHP agonist to the bath. (*C*) Latencies predicted from the MWC model with and without DHP agonists. (*D*) Latencies predicted from Scheme 1 with the same values for parameters A, B, V_S, k_L, and k_{-L}.

In the absence of DHP agonists, the first latencies clearly appeared to be longer. It is, however, difficult to obtain control data over a wide potential range. At positive test potentials ($\geq +10$ mV) threshold crossing schemes were not reliable, due to the low signal to noise ratio. At negative potentials (≤ -10 mV) the latencies were so long that it was not possible to accurately estimate the saturating probability of channel opening. It was possible to measure first latencies in the presence and absence of DHPs at 0 mV in two patches (Fig. 13, *A* and *B*). In each case the first latencies were considerably shortened in the presence of (+) 202-791.

The MWC model predicts such a DHP-induced reduction in the first latencies, as the channel would be more likely to open with fewer than all four voltage sensors in the + position in the presence of DHP agonists (Fig. 13 *C*). Scheme 1 predicts a much smaller effect, as nearly all of the latency is in the voltage-dependent closed–closed steps. In fact, the slight shortening of the first latencies with Scheme 1 (Fig. 13 *D*) is primarily artifactual, as very brief openings which would go unresolved in control conditions will be lengthened and thus detected in the presence of DHPs. According to our simulations, the maximum change predicted by Scheme 1 is too small to explain the observed effect of DHP agonists on the first latency distributions.

Schemes 1 and 2 predict that interburst closed times should get very short at positive voltages. However, the experimental data include long closed times, even with DHP agonists. Such closed states cannot be on the main pathway leading from resting states to the open state, since the first latencies are rapid. We therefore suspect that the long closed times are related to inactivation, and do not consider them further here.

DISCUSSION

Model-independent Results

Since we have chosen to present our results in the context of a novel model, we should indicate the features of the experimental data that do not depend on the model. Gating is not voltage dependent within bursts, so the limiting p(open) is <1 in control conditions. The increase in current with DHP agonists is associated with slower deactivation kinetics, a shift in the activation curve to more negative voltages (with an increase in slope), shorter latencies to first opening, a higher p(open) within bursts, and a higher maximal p(open) at extreme positive voltages. With DHP agonists, open times are bi-exponentially distributed, with long and short openings intermingled. DHP agonists bind and unbind rather slowly, and the open times do not depend on voltage or DHP concentration. The current levels for fully open channels are the same with and without DHPs. Some but not all of these features are familiar from previous studies of calcium channel kinetics in other cell types.

Calcium channel gating is extremely rapid (Fig. 2 *A*), so we were unable to reliably obtain rate constants for channel opening and closing directly from measurement of channel open and closed times, or from noise analysis. However, analysis of point-by-point amplitude histograms shows that the channel is open 50–70% of the time during a burst, and this is not dependent on voltage in the measurable region. The absolute opening and closing rates are less well determined, but as it seems unlikely that both would change in the same direction with voltage, our data imply a

voltage-independent transition between the open state and a closed state. That closed state need not be on the normal pathway for channel opening, but that is the simplest assumption, and the marked decrease in channel closing rate with DHP agonists makes explanations such as channel block unlikely. Voltage-independent intraburst kinetics were also noted by Hagiwara and Ohmori (1983) in pituitary cells.

The voltage independence of kinetics within a burst contrasts sharply with the strong voltage dependence (e-fold for 7.5 mV; Table II) of other measures of calcium channel gating, such as p(open), latencies to first opening, and whole cell kinetics (Figs. 8–10, 12). We estimate that a 50% change in the C-O equilibrium constant could have been detected (Fig. 4, *A* and *B*). Thus, we cannot rule out a weak voltage dependence (e-fold for >40 mV) of the C-O equilibrium, but most if not all of the voltage dependence of calcium channel activation is in the C-C transitions. It seems likely that the microscopic channel opening step and movement of the voltage sensors are qualitatively different processes.

The data under control conditions are consistent with a single open state, but the bursting kinetics clearly indicate at least two closed states, as previously reported (Fenwick et al., 1982; Cavalie, Ochi, Peltzer, and Trautwein, 1983; Brown, Lux, and Wilson, 1984). However, our values for k_L and k_{-L} are considerably faster than previous estimates of the rate constants to and from the open state. This is likely to be due to the effect of missed events in direct measurements of open and closed times, which are severe when both open and closed times are fast. Actually, k_L and k_{-L} could be considerably faster than we estimate, but values more than two times slower would not fit our data well (Fig. 4 *B*). It may seem strange that the best way to measure rate constants of $\sim 10{,}000\ s^{-1}$ is to begin by filtering at 300 Hz, but Koren et al. (1990) also found that a beta distribution analysis was more sensitive than noise analysis for channel gating that was clearly too rapid to measure by threshold-crossing techniques.

Macroscopic currents show a clear delay (Fig. 10), as do distributions of latencies to first opening (Fig. 12), which also indicate the existence of multiple closed states. It is noteworthy that macroscopic activation kinetics were slightly slower with DHP agonists than in control, although the first latencies were considerably faster with DHPs.

Data with DHP agonists require the existence of at least two open states (Fig. 5 *A*). As DHP agonists appear to bind and unbind relatively slowly (Fig. 6), but fast and slow openings can occur in the same sweep (Fig. 7), we conclude that two kinetically distinct open states are available to the DHP-modified channel.

Alternative Models

Scheme 1. This model (Fig. 1 *A*) can explain our data in control conditions and most of the data in DHP-modified conditions if we assume that DHP agonists act to stabilize the open state. According to this scheme DHP agonists would lengthen channel open times, slow deactivation kinetics, and shift the steady-state activation curve in the negative direction while increasing its slope, as we have observed. However, the reduced latencies to first opening and multiple open states observed in the presence of DHP agonists can be explained by Scheme 2 but not Scheme 1.

Activation kinetics. The simplest model worthy of serious consideration for calcium channel activation is a linear C_1-C_2-O model. However, if the C_2-O transition rates are fast and voltage independent, as our data suggest, then the C_1-C_2 transition would be the only voltage-dependent step. Activation would thus be essentially described by a single exponential, with no appreciable lag, contrary to data presented here and elsewhere. A four-state C_1-C_2-C_3-O model (Brown, Tsuda, and Wilson, 1983; Hagiwara and Ohmori, 1983; Taylor, 1988) could better describe our data, but again, if the last transition is voltage independent and fast with respect to the others, the two rate-limiting, voltage-dependent steps would primarily determine the activation kinetics. If we assume independent identical gates, then good fits to current activation require at least three gates. If we relax the requirement that the gates be identical, then this model could explain many of our results. However, such a model has more free parameters (six at any one voltage, and four in order to determine the voltage dependence of the C-C transitions, assuming that C_3-O is voltage independent) than other models considered and bears no relation to any known structural features of the channel.

Dihydropyridines. Several qualitatively distinct models for the actions of DHP agonists have been proposed. Hess et al. (1984) proposed that DHP agonists act to enhance "mode 2" gating of calcium channels, where the channel has an unusually high probability of being open. The channel can be in mode 2 under normal conditions, but DHP agonists greatly increase the proportion of time in mode 2. A mode is thought of as a collection of closed and open states, with transitions among states within a mode much faster than transitions between modes.

Our data favoring slow kinetics for DHP action are consistent with a mode-based model. One interpretation is that our model for normal channel gating is mode 1 of Hess et al. (1984), and gating with k_L and k_{-L} modified by DHP agonists is mode 2. On theoretical grounds, it can be argued that any state of the protein accessible with DHPs bound can also exist without DHPs, but at a higher energy level, which could explain the occasional observation of mode 2 gating under control conditions. We also see rare sweeps with high open probability and long openings without DHP agonists. This was observed in some but not all patches, so we cannot attempt to model this phenomenon here.

Other proposals use more conventional state models for DHP action. Sanguinetti et al. (1986) proposed that DHP agonists simply slow the rate constant for channel closing. This is similar in spirit to our proposal that only the immediate closed–open transition is affected by DHP agonists, but their model cannot explain the DHP agonist-induced decrease in latency to first opening.

The model of Lacerda and Brown (1989) requires very rapid binding of DHP agonists to calcium channels. Their scheme also predicts a concentration dependence of open times, and several distinct single channel conductance levels. We have not observed such phenomena, although a substate of roughly half the normal conductance was seen occasionally in a few patches. Some other features of the data of Lacerda and Brown (1989), including shortened first latencies in the presence of DHP agonists, can be naturally explained by Scheme 2.

Hering et al. (1989) have investigated directly the time course of DHP agonist action by a rapid flow technique. They observed a slow action of 1 μM (+) 202-791

($\tau \sim 1$ s) at -20 mV, with a clear delay, which they attributed to binding of DHP agonists to closed as well as open states of the channel. At 0 mV the action was more rapid ($\tau \sim 400$ ms) and no delay was observed, suggesting more rapid binding to the open state. These effects support our conclusion that the binding of DHP agonists is slow with respect to one of our 135-ms depolarizations. It could be argued that if DHP agonists act by first partitioning into the membrane and then binding to the channel, application of (+) 202-791 via the aqueous medium might produce a slow effect. However, if partitioning into the membrane is the rate-limiting step, the time course should not be voltage dependent.

The model of Hering et al. (1989) assumed that DHP agonists bind equally rapidly to all states of the channel, but DHP-modified channels gate abnormally. We prefer the MWC model, which does imply state-dependent binding, as it allows microscopic reversibility. Their model also required that DHP agonists bind in a voltage-dependent manner, which seems unlikely for nonpolar drugs.

High p(open) gating has been reported for conditions other than binding of DHP agonists, including β-adrenergic agonist action (Yue, Herzig, and Marban, 1990), strong depolarization (Pietrobon and Hess, 1990), and recovery from inactivation (Slesinger and Lansman, 1991). It is possible that these apparently diverse phenomena involve similar effects on k_L and k_{-L}.

Implications of the MWC Model

We have argued that the MWC model (Scheme 2) is consistent with existing information on channel structure, since the main (α_1) subunit of calcium channels is a large protein with four homologous domains, each containing a putative voltage sensor (S4 helix). It might be argued that the MWC model is too simple to be realistic for calcium channels. Calcium channels have additional subunits, which can modulate activation and inactivation kinetics (Singer, Biel, Lotan, Flockerzi, Hofmann, and Dascal, 1991). The four internal repeat domains within α_1 are homologous but not identical. In particular, the S4 regions contain varying amounts of positive charge (Mikami, Imoto, Tanabe, Niidome, Mori, Takeshima, Narumiya, and Numa, 1989). The MWC model could be easily extended to allow asymmetrical behavior of the voltage sensors, but none of our present data requires that. Certainly, many aspects of calcium channel gating (inactivation, voltage-dependent mode switching, channel–channel variability, roles of additional subunits) are beyond the scope of this paper. But we expect that Scheme 2 can serve as a starting point for description of such features of channel gating.

Calcium channels are members of a homologous family of voltage-dependent ion channels. The S4 helix is strongly conserved among these proteins, suggesting that voltage-dependent ion channels share a common gating mechanism. Thus, our model for cooperative gating of the calcium channel may be equally applicable to other voltage-dependent ion channels. It is also likely that other drugs, neurotransmitters, and proteins can act as allosteric effectors of channel gating.

We thank Drs. Keith S. Elmslie, Terrone L. Rosenberry, George R. Dubyak, Masao Ikeda-Saito, and Carlos Obejero-Paz for helpful discussion. We also thank Dr. D. Roemer and Dr. E. Rissi (Sandoz, Basel, Switzerland) for (+) 202-791.

This work was supported in part by NIH grants HL-41206 to Dr. Antonio Scarpa and NS-24471 to S. W. Jones. S. W. Jones is an Established Investigator of the American Heart Association. T. N. Marks was supported by an NIH Medical Scientist Training Program.

Original version received 8 June 1990 and accepted version received 18 November 1991.

REFERENCES

Brown, A. M., H. D. Lux, and D. L. Wilson. 1984. Activation and inactivation of single calcium channels in snail neurons. *Journal of General Physiology.* 83:751–769.

Brown, A. M., Y. Tsuda, and D. L. Wilson. 1983. A description of activation and conduction in calcium channels based on tail and turn-on current measurements in the snail. *Journal of Physiology.* 344:549–583.

Catterall, W. A. 1986. Molecular properties of voltage-sensitive sodium channels. *Annual Review of Biochemistry.* 55:953–985.

Cavalie A., R. Ochi, D. Peltzer, and W. Trautwein. 1983. Elementary currents through Ca^{2+} channels in Guinea pig myocytes. *Pflügers Archiv.* 398:284–297.

Chen, C., and P. Hess. 1990. Mechanism of gating of T-type calcium channels. *Journal of General Physiology.* 96:603–630.

Fenwick, E. M., A. Marty, and E. Neher. 1982. Sodium and calcium channels in bovine chromaffin cells. *Journal of Physiology.* 331:599–635.

Fish, R. D., G. Sperti, W. S. Colucci, and D. E. Clapham. 1988. Phorbol ester increases the dihydropyridine-sensitive calcium conductance in a vascular smooth muscle cell line. *Circulation Research.* 62:1049–1054.

FitzHugh, R. 1983. Statistical properties of the asymmetric random telegraph signal, with applications to single-channel analysis. *Mathematical Biosciences.* 64:75–89.

Galizzi, J.-P., J. Qar, M. Fosset, C. Van Renterghem, and M. Lazdunski. 1987. Regulation of calcium channels in aortic muscle cells by protein kinase C activators (diacylglycerol and phorbol esters) and by peptides (vasopressin and bombesin) that stimulate phosphoinositide breakdown. *Journal of Biological Chemistry.* 262:6947–6950.

Giannattasio, B., S. W. Jones, and A. Scarpa. 1991. Calcium currents in the A7r5 smooth muscle–derived cell line. Calcium-dependent and voltage-dependent inactivation. *Journal of General Physiology.* 98:987–1003.

Hagiwara, S., and H. Ohmori. 1983. Studies of single calcium channel currents in rat clonal pituitary cells. *Journal of Physiology.* 336:649–661.

Hering, S., T. Kleppisch, E. N. Timin, and R. Bodewei. 1989. Characterization of the calcium channel state transitions induced by the enantiomers of the 1,4-dihydropyridine Sandoz 202 791 in neonatal rat heart cells: a nonmodulated receptor model. *Pflügers Archiv.* 414:690–700.

Hess, P., J. B. Lansman, and R. W. Tsien. 1984. Different modes of Ca channel gating behaviour favoured by dihydropyridine Ca agonists and antagonists. *Nature.* 311:538–544.

Hille, B. 1984. Ionic Channels of Excitable Membranes. Sinauer Associates, Inc., Sunderland, MA. 331–334.

Hodgkin, A. L., and A. F. Huxley. 1952. A quantitative description of membrane current and its application to conduction and excitation in nerve. *Journal of Physiology.* 117:500–544.

Horn, R. 1991. Estimating the number of channels in patch recordings. *Biophysical Journal.* 60:433–439.

Koren, G., E. R. Liman, D. E. Logothetis, B. Nadal-Ginard, and P. Hess. 1990. Gating mechanism of a cloned potassium channel expressed in frog oocytes and mammalian cells. *Neuron.* 4:39–51.

Lacerda, A. E., and A. M. Brown. 1989. Nonmodal gating of cardiac calcium channels as revealed by dihydropyridines. *Journal of General Physiology.* 93:1243–1273.

MacKinnon, R. 1991. Determination of the subunit stoichiometry of a voltage-activated potassium channel. *Nature.* 350:232–235.

Marks T. N., G. R. Dubyak, and S. W. Jones. 1990. Calcium currents in the A7r5 smooth muscle-derived cell line. *Pflügers Archiv.* 417:433–439.

McCarthy, R. T., and C. J. Cohen. 1989. Nimodipine block of calcium channels in rat vascular smooth muscle cell lines. Exceptionally high-affinity binding in A7r5 and A10 cells. *Journal of General Physiology.* 94:669–692.

Mikami, A., K. Imoto, T. Tanabe, T. Niidome, Y. Mori, H. Takeshima, S. Narumiya, and S. Numa. 1989. Primary structure and functional expression of the cardiac dihydropyridine-sensitive calcium channel. *Nature.* 340:230–233.

Monod, J., J. Wyman, and J.-P. Changeux. 1965. On the nature of allosteric transitions: a plausible model. *Journal of Molecular Biology.* 12:88–118.

Noda, M., T. Ikeda, T. Kayano, H. Suzuki, H. Takeshima, M. Kurasaki, H. Takahashi, and S. Numa. 1986. Existence of distinct sodium channel messenger RNAs in rat brain. *Nature.* 320:188–192.

Pietrobon, D., and P. Hess. 1990. Novel mechanism of voltage-dependent gating in L-type calcium channels. *Nature.* 346:651–655.

Sanguinetti, M. C., D. S. Krafte, and R. S. Kass. 1986. Voltage-dependent modulation of Ca channel current in heart cells by Bay K8644. *Journal of General Physiology.* 88:369–392.

Singer, D., M. Biel, I. Lotan, V. Flockerzi, F. Hofmann, and N. Dascal. 1991. The roles of the subunits in the function of the calcium channel. *Science.* 253:1553–1557.

Slesinger, P. A., and J. B. Lansman. 1991. Reopening of Ca^{2+} channels in mouse cerebellar neurons at resting membrane potentials during recovery from inactivation. *Neuron.* 7:755–762.

Stevens, C. F. 1978. Interactions between intrinsic membrane proteins and electric field. An approach to studying nerve excitability. *Biophysical Journal.* 22:295–306.

Stühmer, W., F. Conti, H. Suzuki, X. Wang, M. Noda, N. Yahagi, H. Kubo, and S. Numa. 1989. Structural parts involved in activation and inactivation of the sodium channel. *Nature.* 339:597–603.

Taylor, W. R. 1988. Two-suction-electrode voltage-clamp analysis of the sustained calcium current in cat sensory neurones. *Journal of Physiology.* 407:405–432.

Van Renterghem, C., G. Romey, and M. Lazdunski. 1988. Vasopressin modulates the spontaneous electrical activity in aortic cells (line A7r5) by acting on three different types of ionic channels. *Proceedings of the National Academy of Sciences, USA.* 85:9365–9369.

Yellen, G. 1984. Ionic permeation and blockade in Ca^{2+}-activated K^+ channels of bovine chromaffin cells. *Journal of General Physiology.* 84:157–186.

Yue, D. T., S. Herzig, and E. Marban. 1990. β-Adrenergic stimulation of calcium channels occurs by potentiation of high-activity gating modes. *Proceedings of the National Academy of Sciences, USA.* 87:753–757.

Zagotta, W. N., and R. W. Aldrich. 1990. Voltage-dependent gating of *Shaker* A-type potassium channels in *Drosophila* muscle. *Journal of General Physiology.* 95:29–60.